An Analysis on Thermal Energy Storage in Paraffin-Wax Using Tube Array on a Shell and Tube Heat Exchanger

Syukri Himran, Rustan Taraka, Anto Duma

Abstract—The aim of the study is to improve the understanding of latent and sensible thermal energy storage within a paraffin wax media by an array of cylindrical tubes arranged both in in-line and staggered layouts. An analytical and experimental study is carried out in a horizontal shell-and-tube type system during melting process. Pertamina paraffin-wax was used as a phase change material (PCM), while the tubes are embedded in the PCM. From analytical study we can obtain the useful information in designing a thermal energy storage such as: the motion of interface, amount of material melted at any time in the process, and the heat storage characteristic during melting. The use of staggered tubes is proposed compared to in-line layout in a heat exchanger as thermal storage. The experimental study is used to verify the validity of the analytical predictions. From the comparisons, the analytical and experimental data are in a good agreement.

Keywords—Latent, sensible, paraffin-wax, thermal energy storage, conduction, natural convection.

I. INTRODUCTION

THE use of low and high temperature thermal energy storage has been considered in many residential and industrial applications and power plants as well. Low temperature thermal energy storage permits the utilization of alternative energy sources, while high temperature thermal energy storage permits the utilization of waste heat and conservation of premium fuel in all type of power plants.

Among the various type of thermal energy storage medium, latent joined with sensible heat storage is particularly attractive due to its ability to provide high volumetric energy storage and its characteristic to store heat nearly at constant temperature corresponding to the phase change material (PCM) [1]-[5]. During melting process, added heat is stored as latent heat and during freezing this heat is liberated. Since to operate the latent heat system is needed a sufficient temperature gradient above or below the PCM melting point to provide heat transfer, so that latent heat storage also utilize some sensible heat in its operation. However the temperature interval should not be excessive, an interval about 5 to 10°C has been employed for many systems [4].

The PCMs proposed for low temperature applications mostly are both organic and inorganic substances such as paraffin hydrocarbons, paraffin wax and salt hydrates. whereas

SyukriHimran (lecturer), Rustan Taraka (lecturer), Anto Duma (graduate student) is with the Department of Mechanical Engineering, Faculty of Engineering, Hasanuddin University, Makasssar 90245, Indonesia, (Phone: 0411-586015; fax: 0411-586015; e-mail: syukri_h@yahoo.com).

for high temperature applications are either inorganic salts or metals. Among the metals, aluminum, magnesium, and zinc have been mentioned as suitable examples. Most of the metals can be ruled out as PCMs because of their high price, low heat of fusion per unit weight, their possible toxicity and other unfavorable chemical properties [2].

A number of reports on thermal energy storage on TES [1]-[5] have been made where it has been pointed out that PCMs usually have low thermal conductivity. This low thermal conductivity allows only a small heat transfer rate when a melted and a solidified layer of PCM have been formed on the heat exchanger surfaces during heat absorption and heat extraction, respectively. This means that while these materials store or extract thermal energy, it takes a long time or large temperature difference between the heating / coolant fluids and melting temperatures to get the heat to transfer through the phase change materials. In order to eliminate these defects a high surface area to volume ratio is required for the combined container and heat exchanger [6], thus the use of an array of tubes is considered more reliable.

The present study is carried out analytically and experimentally only during melting processes at constant wall temperature in TES using an array of tubes, where the tubes are embedded in PCM. The experimental unit is a horizontal shell-tube heat exchangers. The array of cylindrical tubes is arranged both in in-line and in staggered layouts, as shown on Fig. 1. Each the layout is modeled by three different types of tube spacing. Thus we have nine type of array of cylindrical tubes that be used in the experiment. The tube located in the middle of array is chosen as the domain of study, because that tube obtains heat from various directions of neighbor tubes.

The analysis is based on the conduction as the sole heat transfer mechanism in PCMs. The Pertamina paraffin-wax is used as the PCM and filling the shell side of a-horizontal shell-tube heat exchanger. From the analysis we can obtain some important in formations about the thermal energy transfer parameters in PCM's caused by the tube arrangements.

II. ANALYSIS

The problem involving the TES is the phase change or moving boundary problem. The solution of such problems is inherently difficult because the interface between solid and liquid phases is moving as the latent heat is absorbed or released at the interface; as a result the location of the solid-liquid interface is not known a priori and must be calculated as a part of the solution.
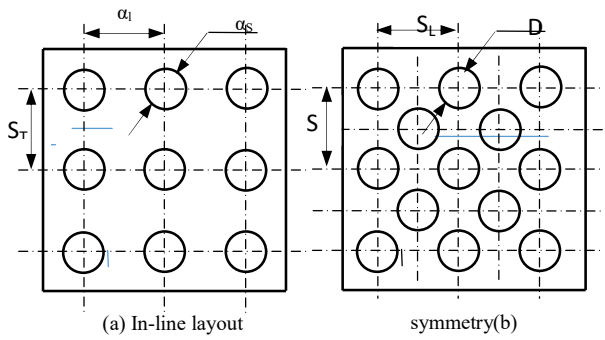
World Academy of Science, Engineering and Technology
International Journal of Aerospace and Mechanical Engineering
Vol:9, No:10, 2015

Fig. 1 In-line and staggered layouts

A. Physical Model and Assumptions

In this conduction is assumed to be the sole heat transport mechanism in PCM. This is a good approximation because of the following reasons:

- During melting process the paraffin wax liquid is viscous.
- The spaces between the heating tubes (filled by PCM) are relatively small.

- During melting process, all the tubes contribute equally to the heat transfer and there is no interaction between them.

Thus, the PCM liquid could be assumed in stable condition and heat transfer through it is by pure conduction.

The heat transfer in PCM of TES is generally a three-dimensional problem, but practically we can assume the heat transfer in the shell-and-tube is two-dimensional. This approximation is acceptable because the tube length is large compared with the tube diameter and tube spacing, so that-the temperature gradient in PCM along the axial direction is much smaller than in the other two directions.

B. Mathematical Model of the Problem

The physical model of the problem can be represented by domain bordered by symmetrical lines as shown in Fig. 2, for in-line and staggered layouts.

By considering the above reasons, the melting problem can be formulated in two-dimensional transient heat conduction, in Cartesian co-ordinate system, consisted of the basic equations; the boundary conditions and initial condition are as follows:
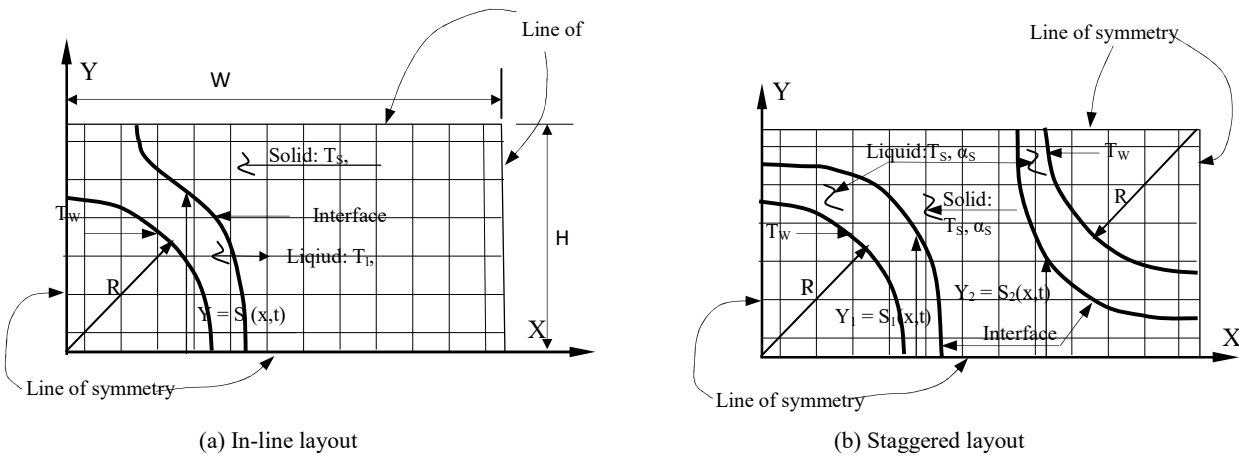

(a) In-line layout   (b) Staggered layout

Fig. 2 Physical model of in-line (a) and staggered (b) layouts

1. Basic Energy Equation [7], [8]:

$$t > 0, : 0 < x < W, S_1(x,t) < y_1 < H, S_2(x,t) < y_2 < H$$

- At liquid phase:

$$\frac{\partial^2 T_l}{\partial x^2} + \frac{\partial^2 T_l}{\partial y^2} = \frac{1}{\alpha_l}\left(\frac{\partial T_l}{\partial t}\right) \quad (1)$$

- At solid phase:

$$\frac{\partial^2 T_s}{\partial x^2} + \frac{\partial^2 T_s}{\partial y^2} = \frac{1}{\alpha_s}\left(\frac{\partial T_s}{\partial t}\right) \quad (2)$$

2. Boundary Conditions [6], $t > 0$:
- At pipe surface: $R = D/2$

$$T_w = T(t) \quad (3)$$

- At interface: $y_1 = S_1(x,t)$, $y_2 = S_2(x,t)$

o Continuity of temperature:

$$T_s = T_l \quad (4)$$

o Energy-balance equation:

$$\left(k_s \frac{\partial T_s}{\partial y} - k_l \frac{\partial T_l}{\partial y}\right)\left[1 + \left(\frac{\partial s}{\partial x}\right)^2\right] = \rho L\left(\frac{\partial s}{\partial t}\right) \quad (5)$$

o At the plane of symmetries:

At $y = 0$ and $y = H$, $\frac{\partial T_s}{\partial y} = 0$ (6)

At $x = 0$ and $x = W$, $\frac{\partial T_s}{\partial x} = 0$ (7)

3. Initial Condition: $t = 0$:

$$T_{PCM} = T_{in}; \ T_w = T(0) \quad (8)$$

World Academy of Science, Engineering and Technology
International Journal of Aerospace and Mechanical Engineering
Vol:9, No:10, 2015

where, $S(x,y,t)$ is the interface position in x,y,t domain, $T_1(x,y,t)$ and $T_s(x,y,t)$ are temperature distributions in the liquid and solid phases, c_{pl}, c_{ps} are heat capacities of liquid and solid phases, α_1 and α_s are thermal diffusivities of liquid and solid phases, respectively. Because of the complexity of the problem, most of the available solution techniques are numerical rather than analytical.

Typically the following thermophysical property of Pertamina paraffin-wax (measured by the Author) is used in experiment and computation in all runs as shown below:

- Transition temperature, T_{tr} = 40.71^{o}C
- Latent heat of transition, L_{tr} = 30080.0 J/kg
- Melting temperature, T_m = 55.0 ^{o}C
- Latent heat of fusion, L = 123300.0 J/kg
- Density: solid, ρ_s = 934.5 kg/m^3
- Density: liquid, ρ_l = 775.0 kg/m^3
- Thermal expansion, β = 0.778 $10^{-3}{}_{70}{}^{o}$C^{-1}
- Specific heat: solid, c_{ps} = 2784.0$_{36.5}$ J/kg.^{o}C
- Specific heat: liquid, c_{pl} = 2080.0$_{72.5}$ J/kg.^{o}C
- Thermal conductivity, k_s = 0.1364 W/m^{o}C
- Kinematic viscosity, υ = 5.234 10^{-6} m^2/s
- Dynamic viscosity, μ = 4.84 10^{-3}Pa.s

Weight composition of the wax can be estimated from Melpolder nomogram [9]: N-alkane: 72%; Iso- and Cyclo-alkane: 28%; average carbon number: 27.5, molecular weight: 387.

These properties are determined by using laboratory measurement, such as differential scanning calorimeter (DSC), calorimeter, and thermal conductivity measuring apparatus. The thermal conductivity measured is only on the solid phase at some temperatures. From the measurement the actual thermal conductivity (k) decreases with the increment of temperature at the solid phase and so is the heat capacity (c_p). But the decreasing of thermal conductivity is more significant than heat capacity. The values of the two properties listed in the table are the average values of those at the temperature span between atmospheric and melting temperature. It also found that the wax has transition and melting temperatures at solid-solid and solid-liquid transformations respectively as shown Fig. 5.

C. Numerical Computation

The method used for numerical solutions are explicit finite difference formulations and expressed in terms of Cartesian coordinates. For convenience, the systems are sub divided into squares. The nodal arrangement is shown in Fig. 3. The notations used in the programming are presented in Fig. 4.

$$q(i,j) = \frac{T(i-1,j)-T(i,j)}{RH(i,j)} + \frac{T(i+1,j)-T(i,j)}{RH(i+1,j)} + \frac{T(i,j-1)-T(i,j)}{RV(i,j)} + \frac{T(i,j+1)-T(i,j)}{RV(i,j+1)} \tag{9}$$

In (10), $q(i,j)$ is the conduction rate in each node, RH is the thermal resistance in horizontal direction, while RV is in vertical direction. The temperature of the node at the next time increment ($t+\Delta t$) is:

$$T'(i,j) = T(i,j) + \frac{q(i,j)}{C(i,j)}\Delta t \tag{10}$$

where $C(i,j)$ is the thermal capacitance of the nodal. To fulfill the explicit numerical stability criterion, an equal time steps Δt have been selected such way that:

$$\alpha \Delta t / \Delta x^2 \leq 1/4 \tag{11}$$

Since the boundary condition at the interface changes due to the absorption of latent heats at the two transformations (solid-solid and solid-liquid), a special technique is used at the two phase transition temperatures. The method was made by monitoring the total energy stored in each node, Fig. 5. When the nodal temperature reached the solid-solid temperature (transition temperature, T_{tr}) and solid-liquid temperature (melting temperature, T_m), the temperature is maintained at this value until sufficient energy was absorbed to balance the transitional or latent heat of the node.

- Q_1 = energy stored by wax node above the initial temperature of wax corresponding to start of phase transition;
- Q_2 = energy stored by wax node above the initial temperature of wax corresponding to the end of phase transition;
- Q_3 = energy stored by wax node above the initial temperature of wax corresponding to start of melting;
- Q_4 = energy stored by wax node above the initial temperature of wax corresponding to the end of phase melting.

The melted fraction of the node, $F(i,j)$, was determined at each time step based on the energy accumulated in the node as:

$$F(i,j) = (Q(i,j) - Q_3)/(\rho \Delta x^2 B\, L) \tag{12}$$

Energy stored in node (i,j), where:

$$Q(i,j) = \sum_{t-1}^{p} \dot{q}(i,j)\Delta t \tag{13}$$

The experimental conditions i.e.: the initial temperature of the PCM, the variations of wall temperature and the period of heating during the melting process are taken into account as the input variables in the numerical computations. The computations are carried out on six configurations of tube layouts, using Fortran IV computer programming. From the computations we can get the heat transfer parameters at each time step:

a. temperature at all nodes,
b. the melted fraction and the position of the interface,
c. the heat stored in each node.

World Academy of Science, Engineering and Technology
International Journal of Aerospace and Mechanical Engineering
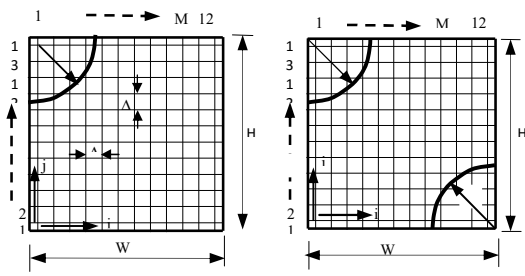Vol:9, No:10, 2015

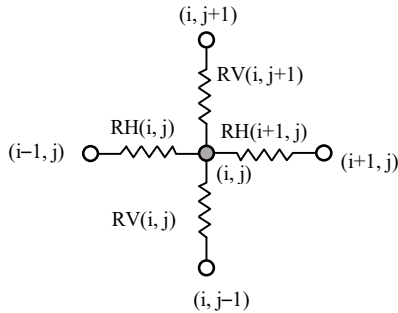Fig. 3 Typical Nodal arrangements of in-line and staggered layouts

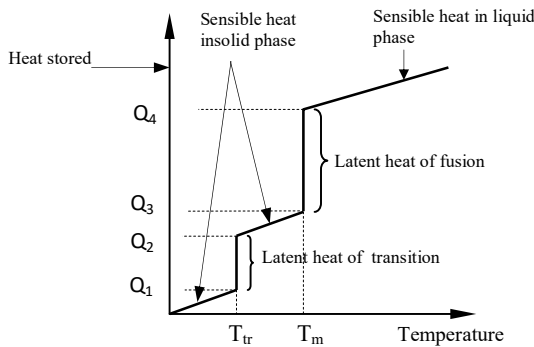Fig. 4 Node notations for finite difference calculations

Fig. 5 A characteristic of heat stored versus temperature for Pertamina paraffin wax

III. APPARATUS AND EXPERIMENTAL PROCEDURE

In this experiment, the effects of an array of cylindrical tubes are studied on the shell-tube container. The tubes are arranged in the in-line and staggered layouts are as shown on Fig. 1. The experimental unit are constructed in six different models of tube arrangements where three types in-line and three types staggered and named as type -1, -2, -3. At each layout, the horizontal tube pitch is kept constant: $S_L = 3D$ while the vertical tube spacing is modified by three kinds of tube distances i.e., $S_T = 3D$, $2D$ and $1.5D$. The tube was made of copper, diameter $D = 1$ inch, and its model length was chosen very large compared to the tube diameter, $L/D = 25.6$. Therefore heat conduction in PCM could be assumed two-dimensional, where the temperature gradients in the axial direction are negligible in comparison with gradients in plane perpendicular to the axis. The tubes are imbedded in paraffin wax as phase change material.

Water as working fluid is heated by using 3 – 4 kW electric heater and circulated around the experimental unit. The experimental apparatus is constructed in such way that when water temperature reaches about 75°C, then it is diverted to the experimental unit, and melting process is started. The desire water mass flow rates are high enough about 0.25 kg/s flowing in each tube to assure the validity of two-dimensional assumption. In order to maintain the constant pipe wall temperature, the voltage of the heater is adjusted by using voltage regulator. The initial temperature of the PCM is at atmospheric temperature or at slightly higher than that.
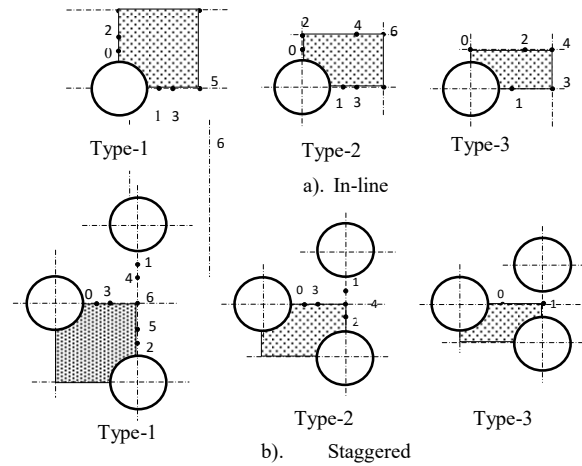

Fig. 6 Measuring points on PCM temperatures during melting process

As many as 10 to 20 T-type thermocouples (Copper - Constantan) are arranged to measure the PCM temperatures during the experiments, where the locations of the measuring points are as shown on Fig. 6. The distance of the point from the surface of the tube at the x-y axis is product of ¼ in (6.35 mm). A pair of points located at x-y axis has same distance from origin. The electric signals from thermocouples in the PCM were received by a computer through data-acquisition software. The tube wall and the inlet/outlet temperatures of water are measured by temperature controller. At 5 minutes interval all the data were recorded. During the experiments the inlet and outlet temperature showed very close value (± 0.1 °C difference) so that the two-dimensional analysis could be implemented. From the experimental measurements we could produce temperature-history of the PCM at various measuring points.

IV. COMPARISONS BETWEEN ANALYTICAL AND EXPERIMENTAL RESULTS

Figs. 7 (a) and (b) show the liquid-solid interfaces and the specific time of occurrence, both for in-line and staggered layout. These movements of interfaces are based on the conduction calculation. The positions of the interface at any time also represent the fraction of melted PCM and the heat stored in PCM.

To check the validity of the theoretical analysis, the analytical and experimental results are compared based on

World Academy of Science, Engineering and Technology
International Journal of Aerospace and Mechanical Engineering
Vol:9, No:10, 2015

temperature-histories of the PCM at the various measuring points as indicated on Fig. 6 for in-line and staggered layouts. All of measuring points are located on the domain study, shown as cross-hatched portion. This domain is nothing other than the physical model of the problem. All the data and the curves of temperature-time histories are available at the author.

Type 1   Type 1

Type 2   Type 2

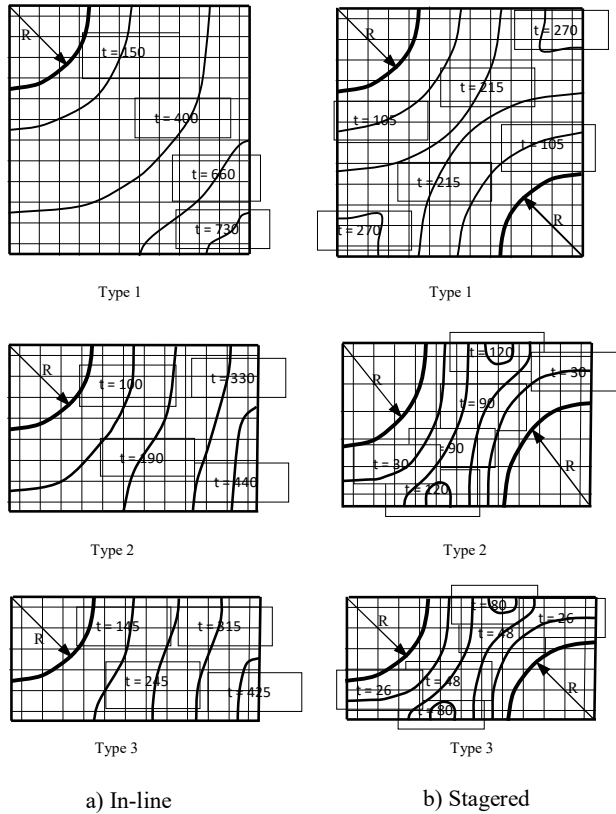Type 3   Type 3

a) In-line   b) Stagered

Fig. 7 Analytical positions of interface at various times (minutes) during melting

Figs. 8 and 9 illustrate temperature-time histories at the selected points for staggered and in-line layouts, the solid line and dotted line represent the calculating and measuring temperature during the melting process. The horizontal line T_m is the melting temperature line and T_w is the wall temperature during the experiment. At the beginning, the curves increase rapidly and then gradually go asymptotically towards melting temperature line. This means at small time t, the heat conduction increases the temperature in the solid phase of the medium as sensible heat storage. The curves demonstrate that the dotted lines are located below the solid lines. This is due to the fact that heat conduction is dominant during melting process. The temperature-time histories at all points and type for staggered layout shows temperature curves of the experiment are always below the heat conduction calculations, similar shapes are as shown on Fig. 8.

The temperature-time histories at the points for in-line type 2 and 3 have the same shape with staggered types, except the points 0, 2, 4 located above top side of the tube for in-line

layout type-1, give a different shape are as indicated on Figs. 9 (a)-(c). These curves show that after several minutes of heating the experimental temperature-time histories deviate from temperature-time histories of heat conduction calculations, where the experimental temperature locate above the calculation temperature. From the experiment, at the period before deviating, interfaces reach the points 0, 2, and 4 after the heating time 275 min's (Fo = 1.076), 365 min's (Fo = 1.428), 435 min's (Fo = 1.702) respectively as shown on Table I. Fourier number Fo=$\alpha t/R^2$, is dimensionless time used to denote the melting time. This stage indicates that, at early times conduction dominates the heat transfer because the conduction temperature-time histories locate above the experimental temperature-time histories. At the time of melting 275 min's, experiment and calculating show that point 0 and 1 reach the melting temperature 55°C at the same time. In addition the liquid region PCM very viscous (μ = 3.80 10^{-2}Pa.s), then we can assume that molten PCM is symmetrical about the axis of the cylinder. At this short period heat conduction dominates, the interface moves uniformly outward as evidenced by the concentric gap. As melting continue the natural convection develops, the plume conveys hot liquid to upper part of the melt region and continues to support the upward movement of the interface. This phenomenon causes the points above tube surface (y-axis) get higher temperatures compared to the points beside tube surface (x-axis) although both the points have same distance from origin. The position of the interfaces at this stage is presented on Fig. 10. The molten PCM is similar to a pear-like shape. The position of the interfaces is constructed by using the ratio between temperature values and distances of the points from the origin.
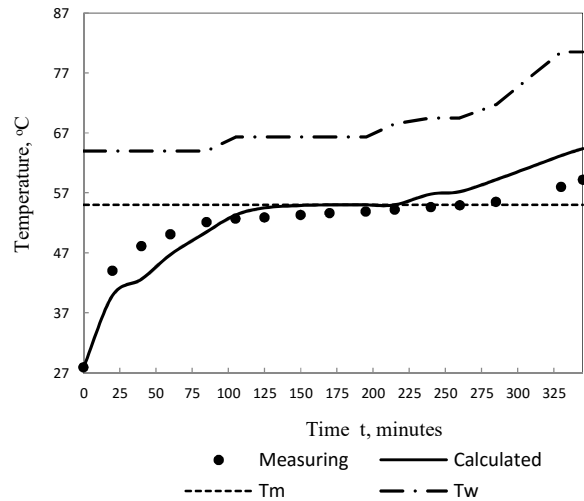

Fig. 8 Experimental and theoretical temperature-time histories of point 2, staggered type-1

Reference [10], on their study i.e.: melting around a horizontal cylinder, clarify that the liquid region is nearly annular at Ste = 0.587 and Fo = 1.92, but our analysis results show Ste = 0.303 and Fo = 1.076. This is due to the heating interaction among the tubes in its layout where the former

World Academy of Science, Engineering and Technology
International Journal of Aerospace and Mechanical Engineering
Vol:9, No:10, 2015

experiment is only carried out on one tubes. The higher Ste and Fo values indicate the higher wall temperature and the longer heating time respectively.
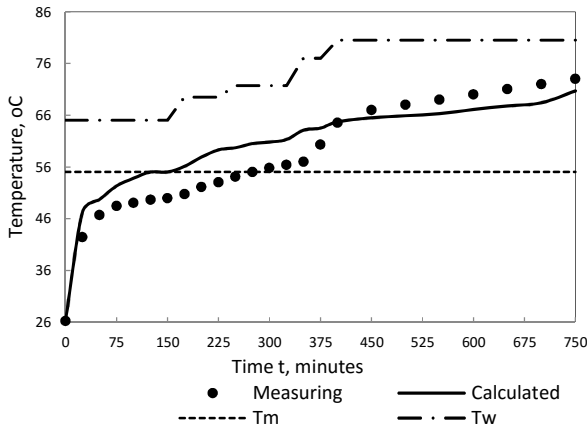
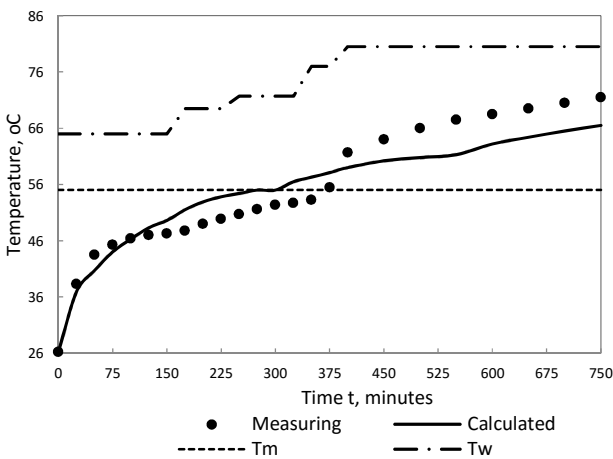Fig. 9 (a) Temperature-time histories of point 0, inline layout, type-1

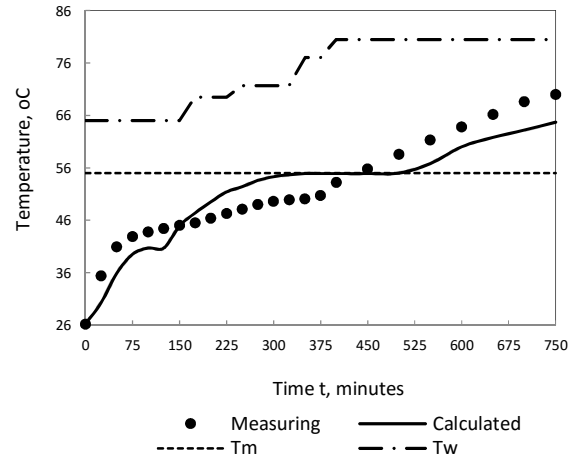Fig. 9 (b) Temperature-time hystories of point 2, in-line type-1

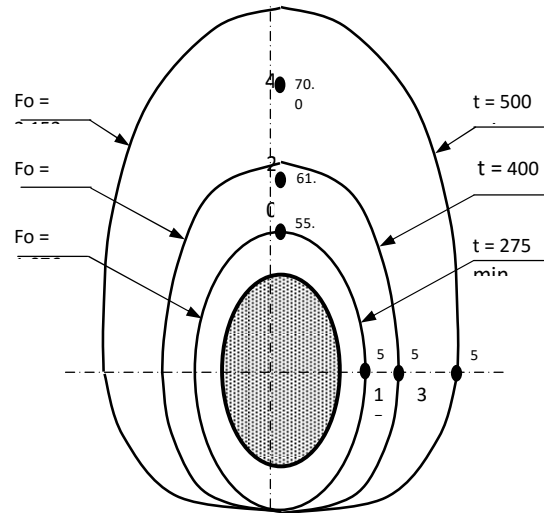Fig. 9 (c) Temperature-time histories of point 4, type 1

Fig. 10 Experimentally determined interface movements

At the time when the tube wall temperature is increased, Stefan number becomes Ste = 0.362, experimental temperature-time histories deviate from temperature-time histories of heat conduction calculations, as shown on Figs. 9 (a)-(c). In this condition, the natural convection is dominant significantly; heat transfer at the upper side of the tubes is very improved and leads to the faster movement of the melting front.

TABLE I
DEVELOPING OF NATURAL CONVECTION

Time (min)	Ste	Fo	$\tau = (Fo*Ste)/(1+Sc)$	Point						
				0	1	2	3	4	5	6
				Temperature °C						
275	0.303	1.076	0.214	55.0	55.0	51.6	51.0	50.7	50.4	49.6
365	0.313	1.428	0.293	59.0	58.5	55.0	53.4	52.8	52.2	51.1
400	0.362	1.565	0.372	64.5	59.1	61.7	55	53.2	52.9	51.8
435	0.362	1.702	0.405	66.3	60.8	65.4	56.1	55.0	53.7	52.6
500	0.362	2.152	0.465	68.0	63.1	66.0	57.8	58.6	55.0	53.2
750	0.362	2.935	0.698	73.0	69.6	71.5	66.6	70	60.5	55.0

World Academy of Science, Engineering and Technology
International Journal of Aerospace and Mechanical Engineering
Vol:9, No:10, 2015

Fig. 11 shows variation of the percentage cumulative melted PCM $F = V_m/V_d$ versus dimensionless time $\tau^* = \frac{F_o \times S_{te}}{S_c}$. Dimensionless time is presented as $\tau^* = F_o.Ste/(1+Sc)$, where sub-cooled condition of the PCM defined by $Sc = \frac{c_{ps}(T_m - T_{in})}{L}$ is included in dimensionless time. From the figures, the staggered layouts give faster melting than the in-line layouts and the staggered with smallest spacing gives the fastest.

Fig. 12 represents variation of the percentage cumulative total heat storage (latent + sensible heat) $Q = Q_s/Q_{max}$ versus dimensionless time for all configurations. According to this figure, against staggered layout gives faster storage of heat than the in-line layout.

From the analysis, in order to eliminate the defect of PCM's low thermal conductivity, we can propose the staggered layout is superior compared to in-line layout for tubes arrangement in shell-and-tube heat exchanger. The use of in-line layout is limited to smaller tube spacing by taking $S_T = 2D$ and $S_L = 3D$.

that $\dot{q}_S$ in liquid phase increases. Total flow rate $\dot{q}_T$ is obtained from Fig. 12, and latent flow rate $\dot{q}_L = \Delta V \times \rho_s \times L/\Delta t$, where ΔV is obtained from the rate of variation in melted paraffin volume V_m in relation to time, as shown in Fig. 11. Both Figs. 13 and 14 give same in formations. The increase of the sensible heat Q_S, and the difference between $\dot{q}_T$ and $\dot{q}_L$, up to t = 60 minutes in Figs. 13 and 14 respectively are due to the sensible heat stored which occurs when the temperature of the solid phase of PCM increases from initial temperature to melting point T_m. The increase of the sensible heat Q_S, the difference between $\dot{q}_T$ and $\dot{q}_L$, after $t = 90$ minutes are due to the sensible heat stored in liquid phase of PCM. In the period between $t = 60$ minutes and $t = 90$ minutes, it may be considered that the heat stores in the PCM approximately the latent heat only, where total heat flow rate $\dot{q}_T$ and latent heat flow rate $\dot{q}_L$ become approximately equal. In the period between t = 0 and t = 48 minutes, the total heat flow rate $\dot{q}_T$ decreases very fast and this is due to the fact that the sensible heat flow rate of solid heat storage in PCM decreases remarkably.
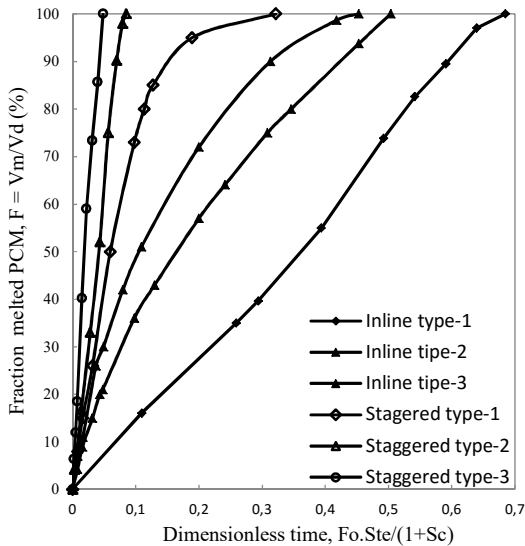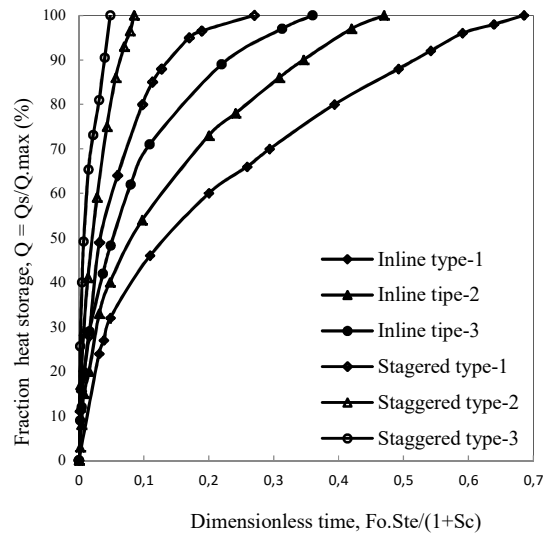

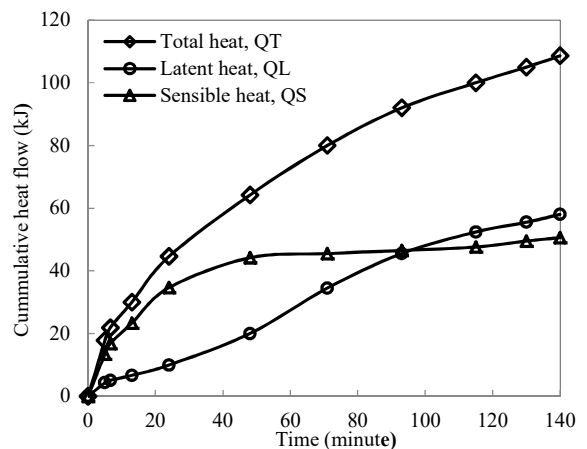Fig. 11 Dimensionless variation of fraction cumulative melted PCM vs dimensionless time

Figs. 13 and 14 demonstrate cumulative, heat flow rate versus time, and give as an example on staggered type-2 layout. Fig. 13 shows a comparison among cumulative heat stored Q_T, which is obtained from Fig. 12, latent heat stored Q_L which is obtained from Fig. 11, and sensible heat stored $Q_S = Q_T - Q_L$. In the period up to t = 60 minutes sensible heat Q_S increase very fast, then, continues to increase slowly. Besides, latent heat stored Q_L increases monotonously in relation to time t.

Fig. 14 shows relation among heat flow rates and time. The total heat flow rate $\dot{q}_T$ shows in the period up to t = 60 minutes, the difference between $\dot{q}_T$ and $\dot{q}_L$ is large, thus sensible heat rate $\dot{q}_S = \dot{q}_T - \dot{q}_L$ in solid phase is large; after that, $\dot{q}_T$ and $\dot{q}_L$ become approximately equal, thus $\dot{q}_S$ is smaller. After $t = 90$ minutes, $\dot{q}_L$ begins to become smaller, this means

Fig. 12 Dimensionless variation of fraction cumulative heat stored vs dimensionless time
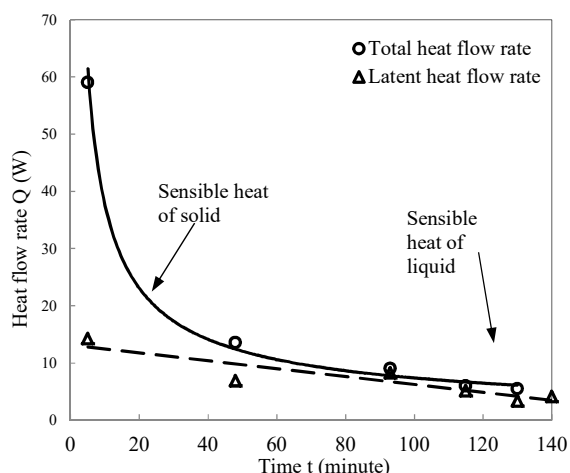

Fig. 13 Typical cumulative heat flow and time

World Academy of Science, Engineering and Technology
International Journal of Aerospace and Mechanical Engineering
Vol:9, No:10, 2015

Fig. 14 Typical heat flow rate and time

NOMENCLATURE

B	Length of the container [m]
c_{pl}, c_{ps}	Specific heat of liquid and solid, respectively [J/kg °C]
D	Tube diameter [m]
$\hat{F}$	Percentage cumulative melted V_m/V_d [%]
Fo	Fourier number, $\alpha_l t/R^2$ [m^2/s]
H	Height, vertical half spacing tube-layout [m]m
k	Thermal conductivity [W/m °C]
L	Latent heat of fusion [J/kg]
q	Heat transfer rate [W]
Q_s	Fraction l heat stored [kJ]
$Q_{s \cdot max}$	Total heat stored [kJ]
Q	Percentage cumulative total heat storage, $Q_s/Q_{s \cdot max}$ [%]
R	Tube radius [m]
RH	Horizontal thermal resistance [°C/W]
RV	Vertical thermal resistance [°C/W]
S	Interface curve position in x,y domain
Sc	Subcooling parameter, $c_{ps}(T_m - Ti)/L$
Ste	Stefan number for melting, $c_{pl}(T_w - T_m)/L$
t	Time [s]
T	Temperature [°C]
V	Volume PCM [m^3]
W	Width, horizontal half spacing tube-layout [m]
x	Coordinate
y	Coordinate

Greek Symbol

α	Thermal diffusivity of PCM, $k/\rho c_p$, [m^2/s]
β	Thermal expansion coefficient [°C]
μ	Dynamic viscosity [Pa.s]
ρ	Density [kg/m^3]
τ^*	Dimensionless time = Fo.Ste

Subscripts

d	Domain
i	Dummy index
in	Initial
j	Dummy index
l	Liquid
L	Latent
m	Melt
s	Solid

REFERENCES

[1] Telkes, M., Solar Energy Storage, *ASHRE* Journal, 1974, pp.38-44.
[2] Kovach, E.G., *Thermal Energy Storage*, Pergamon Press, Oxford, 1976.
[3] Abhat, A., Low Temperature Latent Heat Thermal Energy Storage: Heat Storage Materials, *Solar Energy*, Vol.30, No.41983, pp.313-332.
[4] Lane, G. A., *Solar Heat Storage*: Latent Heat Materials, Vol. II, CRC Press, Inc., Boca Raton, Florida, 1983,pp. 153 – 215.
[5] Himran, S., Suwono A. and Mansoori G. A., Characterization of Alkenes and Paraffin Waxes for Application as Phase Change Energy Storage Medium, *Energy Sources*, Vol. 16, 1994,pp. 117-128.
[6] Wyman, C., Castle, J., and Kreith, F., A Review of Collector and Energy Storage Technology for Intermediate Temperature Applications, *Solar Energy*, Vol. 24, Great Britain, 1980, pp. 517-540.
[7] Ozişik, M.N., *Heat Conduction*, John Wiley & Sons, Inc., New York, NY, 1980, pp. 397-431.
[8] Humphries, W.R. and Griggs, E.I., *A Design Handbook for Phase Change Thermal Control and Energy Storage Devices,* NASA Technical Paper 1074, Science and Technical Information Office, 1977.
[9] Melpolder, F.W., Turner W.R. and Wilbur B.C., A Nomograph for the Estimation of Paraffin Wax Composition, *Tappi*, Vol.47, No.5, 1964, pp.283-285, May.
[10] Bathelt, A. G., Viskanta, R., and Leidenfrost, W., Heat Transfer from Cylinder during Melting of a Thermal Energy Storage Material, *International Heat Transfer Conference*, 6th, Toronto, Canada, 1978,pp. 179 -184, 7-11 August.